

Quantitative volumetric breast density estimation using phase contrast mammography

This content has been downloaded from IOPscience. Please scroll down to see the full text.

View [the table of contents for this issue](#), or go to the [journal homepage](#) for more

Download details:

IP Address: 129.132.210.74

This content was downloaded on 06/09/2015 at 08:38

Please note that [terms and conditions apply](#).

Quantitative volumetric breast density estimation using phase contrast mammography

Zhentian Wang^{1,2}, Nik Hauser³, Rahel A Kubik-Huch⁴,
Fabio D'Isidoro^{1,5} and Marco Stampanoni^{1,2}

¹ Swiss Light Source, Paul Scherrer Institut, 5232 Villigen, Switzerland

² Institute for Biomedical Engineering, University and ETH Zürich, 8092 Zürich, Switzerland

³ Department of Gynecology and Obstetrics, Interdisciplinary Breast Center Baden, Kantonsspital Baden, 5404 Baden, Switzerland

⁴ Department of Radiology, Kantonsspital Baden, 5404 Baden, Switzerland

E-mail: wang@biomed.ee.ethz.ch

Received 19 December 2014, revised 6 March 2015

Accepted for publication 1 April 2015

Published 1 May 2015




Abstract

Phase contrast mammography using a grating interferometer is an emerging technology for breast imaging. It provides complementary information to the conventional absorption-based methods. Additional diagnostic values could be further obtained by retrieving quantitative information from the three physical signals (absorption, differential phase and small-angle scattering) yielded simultaneously. We report a non-parametric quantitative volumetric breast density estimation method by exploiting the ratio (dubbed the R value) of the absorption signal to the small-angle scattering signal. The R value is used to determine breast composition and the volumetric breast density (VBD) of the whole breast is obtained analytically by deducing the relationship between the R value and the pixel-wise breast density. The proposed method is tested by a phantom study and a group of 27 mastectomy samples. In the clinical evaluation, the estimated VBD values from both cranio-caudal (CC) and anterior-posterior (AP) views are compared with the ACR scores given by radiologists to the pre-surgical mammograms. The results show that the estimated VBD results using the proposed method are consistent with the pre-surgical ACR scores, indicating the effectiveness of this method in breast density estimation. A positive correlation is found between the estimated VBD and the diagnostic ACR score for both the CC view ($p = 0.033$) and AP view ($p = 0.001$). A linear regression between

⁵ Current address: Institute for Biomechanics, University and ETH Zürich, 8092 Zürich, Switzerland

the results of the CC view and AP view showed a correlation coefficient $\gamma = 0.77$, which indicates the robustness of the proposed method and the quantitative character of the additional information obtained with our approach.

Keywords: phase contrast imaging, mammography, breast imaging, grating interferometry, volumetric breast density

 Online supplementary data available from stacks.iop.org/PMB/60/104123/mmedia

(Some figures may appear in colour only in the online journal)

1. Introduction

Breast density, namely the relative amount of the fibroglandular tissue versus adipose tissue in the breast, has gained increasing attention in breast cancer screening and diagnosis recently because it has been discussed to be an indicator of the breast cancer risk (Byrne *et al* 1995, Boyd *et al* 2007, Boyd *et al* 2011). The current gold standard for breast density classification is the ACR BI-RADS Breast Density Descriptors, which classify the breast density into four categories (American College of Radiology 2003). The scores are given based on 2D mammograms acquired with screen/film based or digital mammography systems, where the dense fibroglandular tissue and fatty adipose tissue are delineated based on their (sometime subtle) differences in x-ray attenuation (Martin *et al* 2006, Yaffe 2008). This conventional approach has been found to have problems of roughness and subjectivity. Due to the fact that the fibroglandular tissue tends to extend into nearby adipose tissue during the compression of mammographic examination, separating fibroglandular and adipose tissue in a 2D, projective manner is intrinsically difficult. Insufficient inter-reader agreements have been observed in breast density assessments (Nicholson *et al* 2006, Redondo *et al* 2012).

Due to these limitations, there is strong interest in developing methods to measure the volumetric breast density (VBD) (Hartman *et al* 2008, Gweon *et al* 2013), which gives the actual volume of the fibroglandular tissue in the 3D breast volume. VBD is essentially a 3D indicator that could overcome all the limitations of the 2D mammogram-based methods and deliver more accurate results. The most straightforward way to measure the VBD is with 3D breast imaging techniques such as breast computed tomography (CT), which is still at its early period of development, or breast MRI (Thompson *et al* 2009). Other methods, for instance calibration-based methods, dual-energy imaging and phase-shifts-based imaging (Shepherd *et al* 2002, Pawluczyk *et al* 2003, Van Engeland *et al* 2006, Alonzo-Proulx *et al* 2010, Wu *et al* 2012,) have been proposed. Calibration-based methods are easy to implement on conventional mammography systems. However they usually require simultaneous exposure of a calibration phantom alongside the breast and these laborious calibrations will introduce additional complexity in daily mammographic operations.

In this work, based on phase contrast mammography (mammoDPC) (Stampanoni *et al* 2011) we propose a new, non-parametric volumetric breast density estimation method that does not require any pre-calibration. The mammoDPC technology yields three different contrasts of the breast tissue (the conventional absorption, differential phase and small-angle scattering contrasts) simultaneously and has been shown to provide additional clinical values to conventional absorption-based methods (Stampanoni *et al* 2011, Hauser *et al* 2013, Michel *et al* 2013). We used the ratio image of the absorption signal to the scattering signal to classify

Table 1. Diagnostic breast density results of the 27 patients.

ACR score	Description	Number of cases
1	Almost fatty (<25% glandular)	4
2	Scattered fibroglandular densities (25–50% glandular)	13
3	Heterogeneously dense (51–75% glandular)	10
4	Extremely dense (>75% glandular)	0

different tissue combinations of fibroglandular and adipose tissue (Wang *et al* 2013). A corresponding volumetric breast density estimation method is proposed and validated by a phantom study as well as with a dataset obtained from mastectomy samples.

2. Methods

2.1. The mastectomy dataset

This study was approved by the local institutional ethical review board. The mastectomy dataset has been taken from a study on phase contrast mammography recently conducted at Paul Scherrer Institut, Switzerland and Kantonsspital Baden, Switzerland (Stampanoni *et al* 2011, Hauser *et al* 2013). Only samples with small lesion (diameter smaller than 4 cm in the mammograms) have been included in this study to minimize the potential influence to the results caused by the lesions. The samples were imaged using an x-ray Talbot–Lau grating interferometer (David *et al* 2002, Momose *et al* 2003, Pfeiffer *et al* 2006, Pfeiffer *et al* 2008) within 4 h after the surgery to match at best the *in-vivo* situation. The imaging protocol can be found in details in Stampanoni *et al* (2011). 27 samples with known breast density (ACR score) were included. The breast density was scored by experienced radiologists based on subjective assessment on preoperative mammogram according to the ACR BI-RADS Breast Density Descriptors (4th edition). The assessments were obtained *in-vivo* before surgical interventions and therefore are independent from this study. For each sample, two view planes, the cranio–caudal (CC) view and the anterior–posterior (AP) view, were addressed successively, with different compression forces. The CC view is identical to the *in-vivo* situation while the AP view, despite not accessible *in-vivo*, is simple to obtain with excised samples and therefore has been included in our evaluation. The diagnostic ACR scores of the 27 samples are listed in table 1 and were used as the ‘ground-truth’ for the comparison. It is worth mentioning, however, that the ACR scores do not reflect the real breast densities because of the potential subjectivity and intrinsic inaccuracy of the density estimation method. At the time that this paper is under reviewing, ACR BI-RADS (5th edition) starts to be deployed in the clinical routines. The ACR scores 1–4 in the 4th edition are replaced by an equivalent classification using ACR scores a–d in the 5th edition. However, since the patients were diagnosed based on the ACR BI-RADS (4th edition), the lexicon of the 4th edition is used in this paper.

2.2. The Talbot–Lau grating interferometer

The Talbot–Lau grating interferometer was set up at the Paul Scherrer Institut, Villigen, Switzerland. It consists of a Seifert ID 3000 x-ray generator (operated at 40 kVp with mean energy of 28 keV and a current of 25 mA), a three-gratings interferometer (with pitches of $p_0 = 14 \mu\text{m}$, $p_1 = 3.5 \mu\text{m}$ and $p_2 = 2.0 \mu\text{m}$), and a Hamamatsu C9732DK flat panel CMOS detector

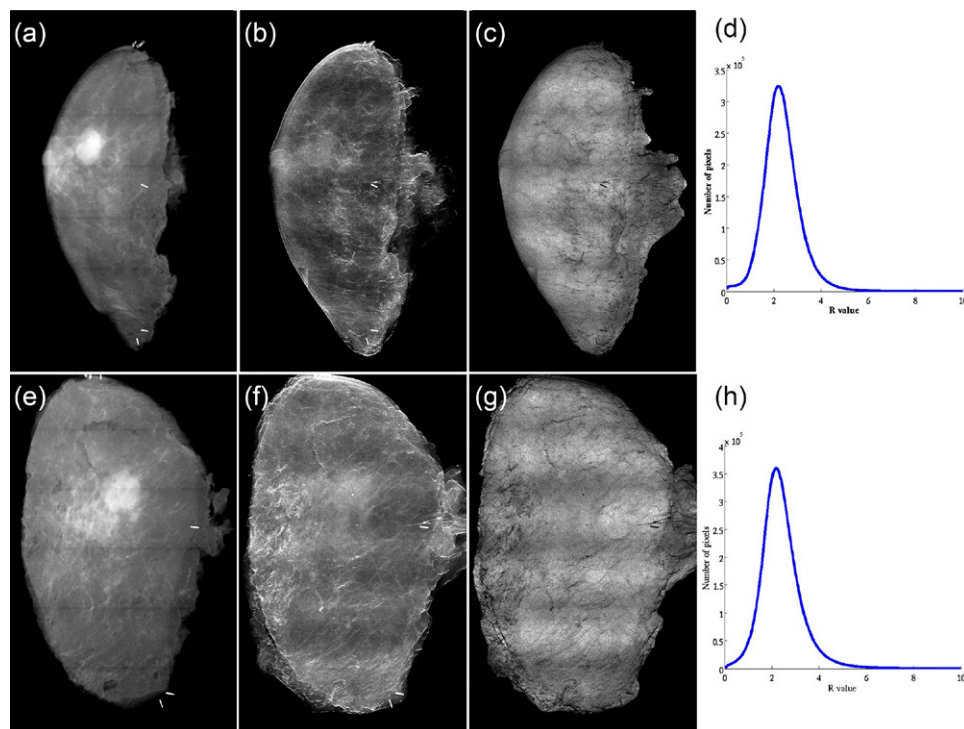


Figure 1. The mammoDPC dataset for a typical case: The conventional absorption image (A), the small-angle scattering image (B) and the corresponding R image (C) in CC view. The sizes of all the images are 5000×7000 pixels. The histogram of the R image is given in (D), which has an asymmetric Gaussian distribution. (E) ~ (H) are the corresponding figures for the AP view of the same sample.

featuring a 50×50 micron² pixel size. The interferometer was tuned at the 5th Talbot distance. The distance from the source to the sample grating was about 140 cm and the source-detector distance was 160 cm. More details regarding the system can be found in (Stampanoni *et al* 2011).

2.3. The breast density phantom

Additional to the mastectomy dataset, a breast density phantom (supplemental digital content SDC1) (stacks.iop.org/PMB/60/104123/mmedia) was also designed and fabricated to evaluate the proposed method. The phantom has a fixed size of 5×5 cm which covers most of the field of view (FOV) and contains exchangeable plastic plates with different thicknesses. It simulates breast compositions of 0%, 20%, 40%, 60%, 80%, 100% fibroglandular tissue and total compression thicknesses of 2, 3, 4 and 5 cm. To the best of our knowledge, there are no suitable materials available that can mimic the fibroglandular and adipose tissue in both absorption and scattering properties simultaneously. In our previous work (Wang *et al* 2013), the material properties of Teflon, PMMA and Nylon have been studied. It has been shown that Nylon and PMMA can be used qualitatively to simulate fibroglandular and adipose tissue. The Nylon–Teflon pair has the same signal behavior as the Nylon–PMMA pair (figures 1 (E)–(F) in Wang *et al* 2013). Here we used Nylon and Teflon to simulate the adipose and fibroglandular tissue, respectively. Although the absolute values are not exactly the same, their relative absorption and scattering properties were observed to have similar behaviors as those

of the adipose and fibroglandular tissue, which makes them the acceptable candidates for a proof-of-concept study.

2.4. The working principle of the R image

We focus on the absorption and small-angle scattering signals obtained in phase contrast mammography. For single materials, these two signals can be approximately expressed by (Heine and Behera 2006, Wang *et al* 2013)

$$A \approx \mu_{\text{eff}}(\bar{E}) \cdot T, \quad (1)$$

$$S \approx s_{\text{eff}}(\bar{E}) \cdot T, \quad (2)$$

respectively. T is the thickness of the material, $\mu_{\text{eff}}(\bar{E})$ is its effective attenuation coefficient and $s_{\text{eff}}(\bar{E})$ is its effective scattering parameter (Wang *et al* 2009) at the mean energy \bar{E} .

We define the R image as the ratio of equations (1) to (2),

$$R = \frac{A}{S} = \frac{\mu_{\text{eff}}(\bar{E})}{s_{\text{eff}}(\bar{E})}. \quad (3)$$

R is thereby the measurable quantity in phase contrast mammography and is independent from the thickness T , which is usually the unknown parameter in radiographic applications. The R value can be considered as the signature of a material in radiology. The same material is expected to show the same R value regardless of the thickness. The mammoDPC images and the corresponding R image for a typical case are shown in figure 1. This sample has a diagnostic breast density of ACR 1. To obtain the relative R value of fibroglandular and adipose tissue, glandular- and adipose- dominant areas are identified from the attenuation images for all the samples. The corresponding areas in the scattering and R images can be easily located, as all images are intrinsically registered on a pixel-by-pixel base. We observed that fibroglandular tissue gives higher attenuation and scattering signals than adipose tissue, but have a smaller R value compared to the adipose tissue.

A possible factor which could invalidate equations (1) and (2) is the beam hardening effect which is particularly pronounced when imaging high-absorbing materials, such as metal or large-scale samples. In mammography, it has been shown that the beam hardening effect for the attenuation signal as well as for the scattering signals is negligible for sample thickness up to 5 cm (Kaufhold *et al* 2002, Heine and Behera 2006, Wang *et al* 2013), therefore equations (1) and (2) holds in a wide sense.

2.5. Volumetric breast density (VBD) estimation using the R image

In this section, we deduce the connection between the R value and the VBD of the breast. On a pixel basis, the VBD can be defined as (Martin *et al* 2006, Wu *et al* 2012)

$$m(x, y) = \frac{T_g}{T} = \frac{T_g}{T_g + T_a}, \quad (4)$$

where T_g and T_a are the thicknesses of the fibroglandular tissue and adipose tissue along the x-ray beam path, respectively. $T = T_g + T_a$ is the total compression thickness. The VBD of the whole breast can be obtained by averaging $m(x, y)$ throughout the whole breast region.

With the two-material breast composition assumption, equation (3) becomes

$$R = \frac{A}{S} = \frac{\mu_g T_g + \mu_a T_a}{s_g T_g + s_a T_a} = \frac{\mu_g m T + \mu_a (1 - m) T}{s_g m T + s_a (1 - m) T} = \frac{\mu_g m + \mu_a (1 - m)}{s_g m + s_a (1 - m)}. \quad (5)$$

Unlike other VBD estimation methods (Wu *et al* 2012) that require knowing the total compression thickness, equation (5) is independent from T , and thereby avoids the potential errors caused by the uncertainty of T . Taking equation (4) into equation (5), the connection between the pixel-wise VBD (m) and the measured quantity R is then set up (Wang *et al* 2013),

$$m(R) = \frac{1}{1 - \frac{\left(\frac{R}{R_g} - 1\right)}{\left(\frac{R}{R_a} - 1\right)} \cdot \frac{\mu_g}{\mu_a}}, R_g < R < R_a \quad (6)$$

where $R_g = \mu_g/s_g$ and $R_a = \mu_a/s_a$ are defined as the R values for 100% fibroglandular tissue and 100% adipose tissue, respectively. In this paper, we define equation (6) as the weighting curve.

The value μ_g/μ_a is actually a constant for a given energy and can be determined by tabulated data (Johns and Yaffe 1987). In our system, the design energy (mean energy) is 28 keV and the corresponding value of $\mu_g/\mu_a = 1.49$ is used in the following sections. Detailed calculations are provided in supplemental digital content SDC2 (stacks.iop.org/PMB/60/104123/mmedia).

In order to get a quantitative value of the VBD from equation (6), R_g and R_a need to be determined. This can be done automatically from the histogram of the R image (denote as $H(R)$). The histogram $H(R)$ is an 'asymmetric Gaussian distribution' (for instance, can be seen from figures 1 (D) and (H)) due to the fact that the adipose tissue (the right part of the histogram) is more dominant in the breast compared to the glandular tissue (the left part) (Yaffe *et al* 2009). The VBD information of the breast can be evinced from the asymmetric distribution of the histogram. The skewness (the third moment) of the distribution can give a good estimation of how dominant either the fibroglandular or the adipose tissue is in the whole breast.

Due to the tissue overlapping in the radiographic images, only a very small amount of pixels can measure pure adipose or fibroglandular tissue. This fact indicates that R_g and R_a can be decided at the margins of the histogram distribution. We determine R_g and R_a from the histogram $H(R)$ in a statistical way by the following steps, which are also illustrated in figure 2:

- Find the peak position R_{peak} from the histogram, which gives the maximal $H(R)$.
- The histogram $H(R)$ is then divided into the left and right parts by R_{peak} . These two parts are considered separately. For each half, the distribution is mirrored around the peak position to form a symmetric Gaussian distribution. Then standard Gaussian fittings are applied to the two resulting distributions and their standard deviations σ_g and σ_a are calculated respectively.
- R_g and R_a are then obtained following the 3σ criterion, i.e. by setting

$$\begin{aligned} R_g &= R_{\text{peak}} - 3\sigma_g \\ R_a &= R_{\text{peak}} + 3\sigma_a \end{aligned} \quad (7)$$

The 3σ criterion covers 99.7% of the area of the histogram and gives a good estimation of the R_g and R_a in the presence of noise.

With R_g and R_a , from equation (7), the VBD of the whole breast can be calculated by weighting the histogram $H(R)$ using equation (6), yielding:

$$VBD = \frac{\sum_R m(R) \cdot H(R)}{\sum_R H(R)}. \quad (8)$$

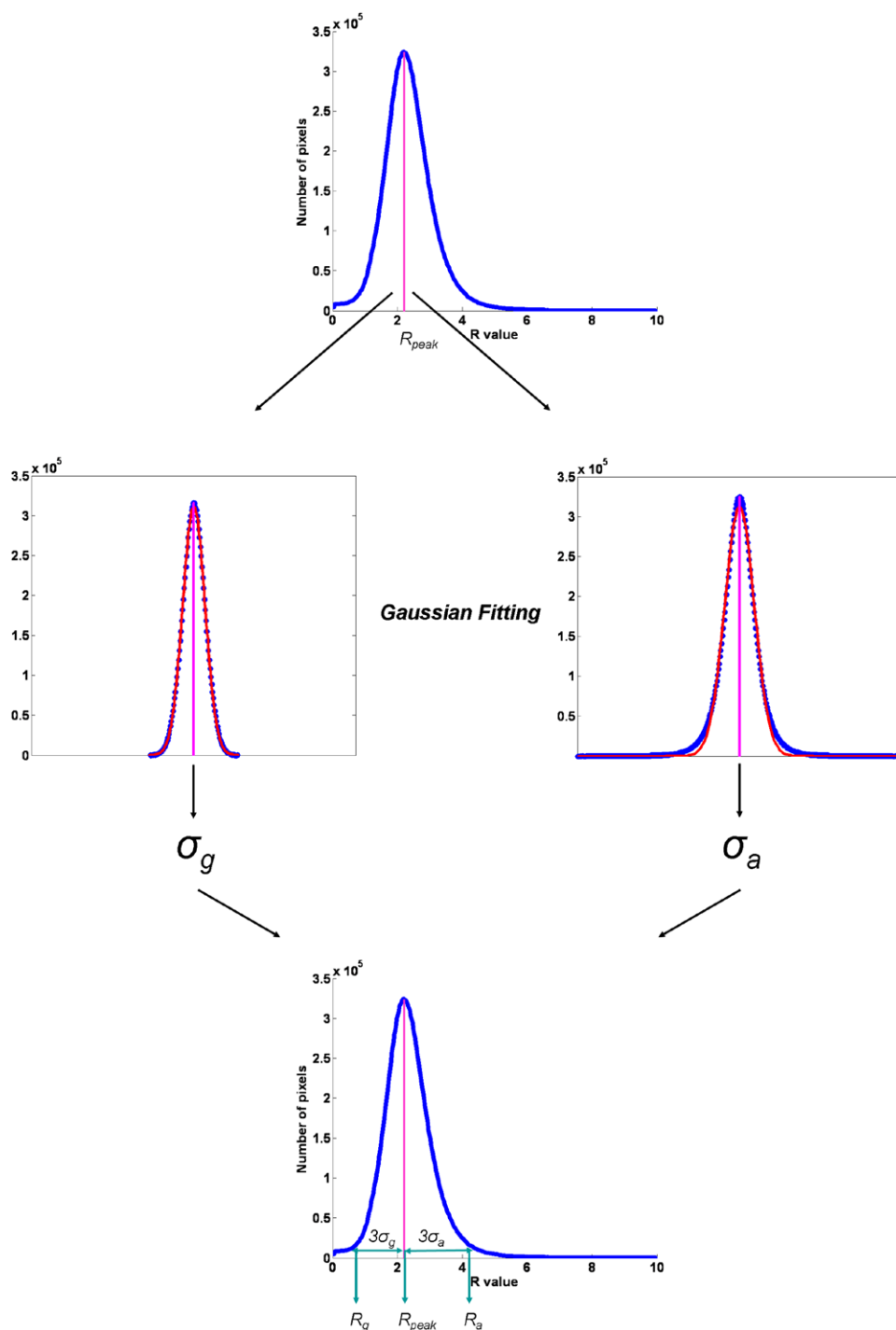


Figure 2. Steps to determine R_g and R_a from the histogram of the R image.

Only the breast area contributes to the histogram $H(R)$: this is achieved via a mask, obtained by thresholding the absorption image, and subsequently applying it to the R image. In this paper, the histograms are obtained using off-the-shelf Matlab function *hist()* with 256 bins.

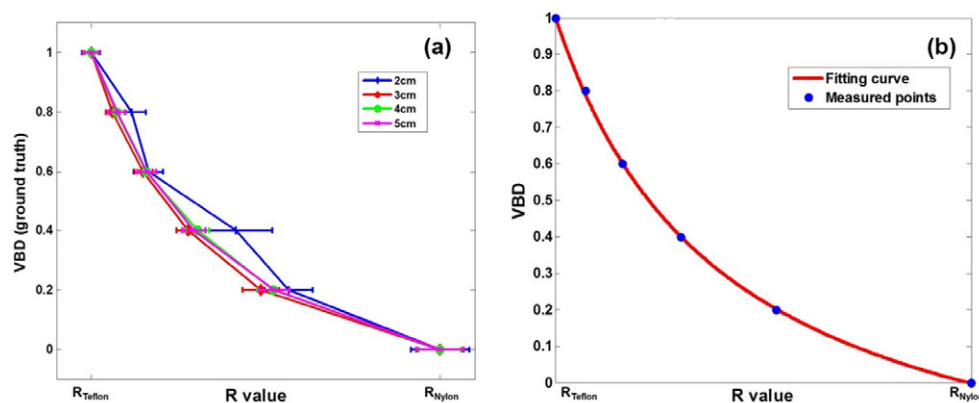


Figure 3. The results of the breast density phantom study. (A) The measured weighting curves for compression thicknesses of 2, 3, 4 and 5 cm. The error bars show the standard deviation for each measured R value. (B) The fitting results for the measurement of compression thickness of 5 cm. The measured points fit the weighting curve model equation (6) very well with an R -squared coefficient of 0.9997.

3. Results

3.1. Breast density phantom study

In this section, we validated the physical model (equation (6)) of the proposed method. Breast density phantoms with thicknesses of 2, 3, 4 and 5 cm were measured. For each thickness, VBDs of 0%, 20%, 40%, 60%, 80%, 100% were simulated using different combinations of the plates and the values are used as the ground truth. In this case, the R values of Teflon and Nylon can be directly measured using the combinations with only Teflon or Nylon. A ROI (600 pixels \times 600 pixels) from the center of the absorption and scattering images was chosen and the R values of the two materials were determined by taking the average over the whole ROIs. The measured R values for Teflon and Nylon are 1.9 and 5.3, respectively.

Figure 3(A) shows the measured weighting curves for different thicknesses and compositions. As can be seen, those curves are overlapping with each other, indicating that the proposed method is independent from the compression thickness. The small inconsistency of the curve for the 2 cm thick phantom is due to the low signal to noise ratio in the R image for this thin phantom. To validate the proposed method, we fitted the measured data for different compositions of the 5 cm thick phantom with the physical model of equation (6), and the results are shown in figure 3(B). The measured data fit the theoretical model with an R -squared coefficient of 0.9997.

3.2. Clinical evaluation

The estimated VBD results from both the CC and AP views are illustrated in figure 4 and the numerical values are summarized in table 2. A few selected cases are shown in supplemental digital content SDC3 (stacks.iop.org/PMB/60/104123/mmedia). The compressed thicknesses of the samples in CC view range from 2.1 to 4.0 cm with a mean value of 3.1 cm; the thicknesses in AP view are from 1.2 to 3.3 cm with a mean value of 2.4 cm. First of all, it is worth mentioning that the calculated VBD values fall in the range of 10% ~ 30%. This is consistent with the results of the previous, independent studies using x-ray tomography (Yaffe *et al*

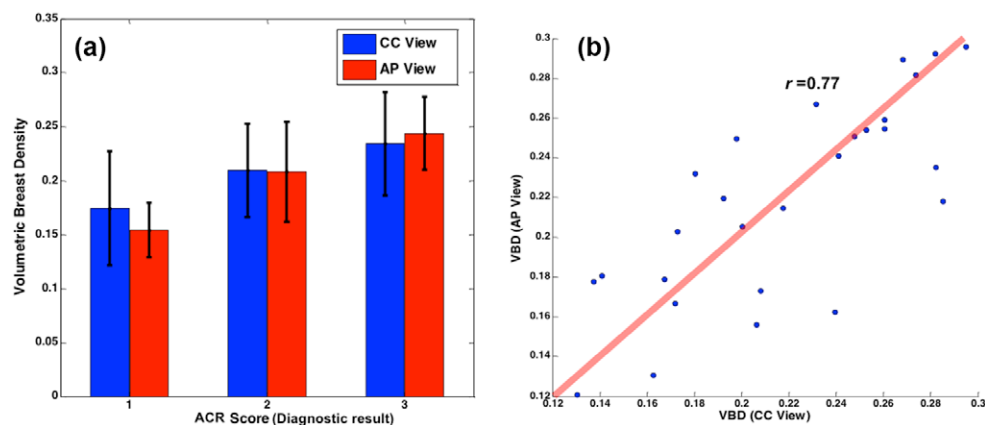


Figure 4. The VBD estimation on 27 mastectomy breast samples. (A) The mean and standard variance of VBD values estimated from CC view and AP view for each group with the same diagnostic ACR score. The mean VBD for each group increases as the diagnostic ACR score gets larger, which indicates that the results of the proposed method are consistent with the diagnostic results. (B) The correlation between the VBD results estimated by the CC view and the AP view. Blue dots represent the individual cases. The linear regression shows a correlation coefficient of 0.77.

Table 2. The estimated VBD results of the 27 samples for each ACR group.

ACR score	Mean VBD	Standard variance
CC View		
1	18%	5%
2	21%	4%
3	24%	5%
AP View		
1	16%	2%
2	21%	5%
3	25%	3%

2009). It can be seen in figure 4(A) that the mean VBD value for each ACR group increases as the diagnostic ACR score increases. This positive correlation holds for both CC view and AP view datasets, and indicates that the proposed method can result in consistent results compared to clinical approach. The standard one-way ANOVA analysis (using *R* statistics (R Core Team 2003) with a confidence interval of 0.95) shows that the estimated VBD values using the proposed method are significantly distinguishable between different diagnostic ACR groups, using CC view dataset ($p = 0.033 < 0.05$), AP view dataset ($p = 0.001 < 0.05$) or CC view and AP view together ($p = 0.000 < 0.05$). This result further confirms that the proposed method is consistent and compatible with the ACR scoring.

Theoretically, the CC and AP views should give the same results for the individual case. Practically however, these two views were taken consecutively with slightly different sample positions, resulting in a different magnification factor on the detector. This obviously affected the estimation of VBDs. In addition, the diffusion of the blood and the breast deformation during the imaging are also expected to induce errors. Despite these limitations, the linear regression between the VBD values obtained in CC and AP view

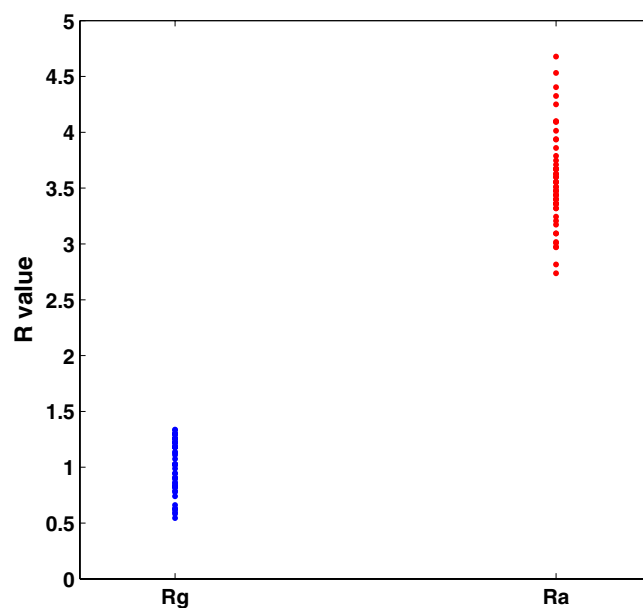


Figure 5. The distribution of the estimated R_g and R_a for samples in the CC view and the AP view. The mean value of R_g is 1.02 and the standard deviation is 0.23; the mean value of R_a is 3.55 and the standard deviation is 0.42.

shows a good correlation coefficient of 0.77 (figure 4(B)), which confirms the robustness of the proposed method.

The distribution of the estimated R_g and R_a for the 27 samples is showed in figure 5. The mean value of R_g is 1.02 and the standard deviation is 0.23, and the mean value of R_a is 3.55 and the standard deviation is 0.42.

The goodness of the Gaussian fitting is evaluated by the relative root mean square (rRMS) between the fitting result and the original histogram, which is defined by $\text{rRMS} = \text{RMS}(\bar{H}(R) - H(R)) / \max(H(R))$. $\bar{H}(R)$ and $H(R)$ are the fitted histogram and raw histogram, respectively, $\text{RMS}()$ is the root mean square function and $\max(H(R))$ is the maximal value of $H(R)$. The rRMS for all the fittings ranges from 0.2 to 2.6% with the mean value of 1.1%, indicating a good fitting for all the cases.

4. Discussion

The good correlation of the VBD values obtained from the AP and CC views supports well the validity of proposed method, in particular when considering that the two views have been acquired independently, under slightly different sample positions and with different compressions. The correlation coefficient is not pronouncedly high, most possibly due to the aforementioned non-ideal experimental conditions. However, it is still a strong indicator that the calculated VDB is a robust, physical quantity that does not depend too much on the experimental conditions.

Our method relies on the fact that the mammographic images are usually large enough, providing sufficient statistics to perform the histogram analysis described in the method section. It has been shown that the intrinsic noise properties of the absorption and scattering images in grating interferometry are different (Revol *et al* 2010). The scattering image tends

to be noisier than the absorption image (Chabior *et al* 2011). Consequently, the ratio—the R image—is also correspondingly noisy. As can be expected, if the mammographic image is very small, the Gaussian fitting will not work properly, resulting in inaccurate R_g and R_a and consequently an unreliable VBD value. However, state-of-the-art mammography equipment provides images with around 6000×4000 pixels. This large pixel counts (24 M pixels) is the key to statistically reliable results even when the R image is relatively noisy. It is also worth mentioning that the proposed method works with other technologies where the absorption and scattering signals of the sample are available, such as diffraction enhanced imaging (DEI) (Chapman *et al* 1997, Wernick *et al* 2003).

At this stage, the study only included a few ($n = 27$) postsurgical breast samples. Although they were not fixed and were imaged immediately after resection, we are aware that they still differ from *in-vivo* breast tissue, mainly because they are not perfused. However, there are no indications that the non-perfused breast will cause significant breast density changes. Actually, this effect should be considered to be negligible as the breast density is mainly affected by the fibroglandular and adipose tissue whereas the blood only takes up a small contribution.

Due to the limited field of view on our experimental system, images of the full breast are obtained by stitching several smaller images together. The background of each acquisition is not perfectly uniform which causes ‘venetian-blind’ artefacts in the R image as can be seen in figure 1. These artefacts may introduce errors in the absolute VBD numbers. Once large field of view and better quality gratings will be available, this artefact will disappear and the proposed algorithm is expected to be more accurate.

Conventional 2D full-field mammography has the intrinsic disadvantage of tissue overlapping; therefore developments towards 3D breast imaging are the logical consequence. Breast CT is still at its early stage, struggling with patient dose management, spatial resolution and contrast issues, while quasi-3D techniques such as breast tomosynthesis have emerged and became mature (Skaane *et al* 2013). In a long-term perspective, we believe that breast phase contrast CT will probably be the ultimate solution. Besides the benefits (fully 3D, isotropic resolution) from the CT mode, it has the potential to significantly reduce patient dose by imaging at a higher energy while still being able to keep sufficient contrast (yielded by the phase information) for diagnosis. Since technical difficulties, such as fabrications of gratings remain challenging, 2D phase contrast mammography is considered to be a reasonable transition and the proposed VBD estimation method could add additional value to phase contrast mammography investigations.

5. Conclusion

In this paper, we introduce a novel, non-parametric volumetric breast density method using gratings-based differential phase contrast mammography. We demonstrated that the new method yields consistent results with clinical diagnostic methods on a non-fixed, whole mastectomy dataset. Our approach is believed to provide more accurate, quantitative information regarding the breast density, eliminating the subjectivity of the current methods. The next step will be to evaluate the presented method applied to *in-vivo* measurements and compare with breast tomographic data where the actual volumetric breast density can be obtained.

References

- Alonzo-Proulx O, Packard N, Boone J M, Al-Mayah A, Brock K K, Shen S Z and Yaffe M J 2010 Validation of a method for measuring the volumetric breast density from digital mammograms *Phys. Med. Biol.* **55** 3027–44

- American College of Radiology 2003 *Breast Imaging Reporting and Data System (BI-RADS)* 4th edn (Reston, VA: American College of Radiology)
- Boyd N F et al 2007 Mammographic density and the risk and detection of breast cancer *New Engl. J. Med.* **356** 227–36
- Boyd N F, Martin L J, Yaffe M J and Minkin S 2011 Mammographic density and breast cancer risk: current understanding and future prospects *Breast Cancer Res. Treat.* **13** 223
- Byrne C, Schairer C, Wolfe J, Parekh N, Salane M, Brinton L A, Hoover R and Haile R 1995 Mammographic features and breast cancer risk: effects with time, age, and menopause status *J. Nat. Cancer Inst.* **87** 1622–9
- Chabior M, Donath T, David C, Schuster M, Schroer C and Pfeiffer F 2011 Signal-to-noise ratio in x-ray dark-field imaging using a grating interferometer *J. Appl. Phys.* **110** 053105
- Chapman D, Thomlinson W, Johnston R E, Washburn D, Pisano E, Gmür N, Zhong Z, Menk R, Arfelli F and Sayers D 1997 Diffraction enhanced x-ray imaging *Phys. Med. Biol.* **42** 2015–25
- David C, Nöhammer B, Solak H H and Ziegler E 2002 Differential x-ray phase contrast imaging using a shearing interferometer *Appl. Phys. Lett.* **81** 3287–9
- Gweon H M, Youk J H, Kim J A and Son E J 2013 Radiologist assessment of breast density by BI-RADS categories versus fully automated volumetric assessment *AJR Am. J. Roentgenol.* **201** 692–7
- Hartman K, Highnam R, Warren R and Jackson V 2008 Volumetric assessment of breast tissue composition from FFDM images *Digital Mammography* ed E Krupinski (Berlin: Springer) vol 5116 pp 33–9
- Hauser N et al 2013 A study on mastectomy samples to evaluate breast imaging quality and potential clinical relevance of differential phase contrast mammography *Invest. Radiol.* **49** 131–7
- Heine J J and Behera M 2006 Effective x-ray attenuation measurements with full field digital mammography *Med. Phys.* **33** 4350–66
- Johns P C and Yaffe M J 1987 X-ray characterisation of normal and neoplastic breast tissues *Phys. Med. Biol.* **32** 675–95
- Kaufhold J, Thomas J A, Eberhard J W, Galbo C E and Trotter D E 2002 A calibration approach to glandular tissue composition estimation in digital mammography *Med. Phys.* **29** 1867–80
- Martin K E, Helvie M A, Zhou C, Roubidoux M A, Bailey J E, Paramaql C, Blane C E, Klein K A, Sonnad S S and Chan H P 2006 Mammographic density measured with quantitative computer-aided method: comparison with radiologists' estimates and BI-RADS categories *Radiology* **240** 656–65
- Michel T et al 2013 On a dark-field signal generated by micrometer-sized calcifications in phase-contrast mammography *Phys. Med. Biol.* **58** 2713–32
- Momose A, Kawamoto S, Koyama I, Hamaishi Y, Takai K and Suzuki Y 2003 Demonstration of x-ray Talbot interferometry *Japan. J. Appl. Phys.* **42** L866–8
- Nicholson B T, LoRusso A P, Smolkin M, Bovbjerg V E, Petroni G R and Harvey J A 2006 Accuracy of assigned BI-RADS breast density category definitions *Acad. Radiol.* **13** 1143–9
- Pawluczyk O, Augustine B, Yaffe M J, Rico D, Yang J, Mawdsley G E and Boyd N F 2003 A volumetric method for estimation of breast density on digitized screen-film mammograms *Med. Phys.* **30** 352–64
- Pfeiffer F, Bech M, Bunk O, Kraft P, Eikenberry E F, Brönnimann Ch, Grünzweig C and David C 2008 Hard-x-ray dark-field imaging using a grating interferometer *Nat. Mater.* **7** 134–7
- Pfeiffer F, Weitkamp T, Bunk O and David C 2006 Phase retrieval and differential phase-contrast imaging with low-brilliance x-ray sources *Nat. Phys.* **2** 258–61
- R Core Team 2003 R: a language and environment for statistical computing. R foundation for statistical computing (Vienna, Austria) (www.R-project.org)
- Redondo A, Comas M, Macià F, Ferrer F, Murta-Nascimento C, Maristany M T, Molins E, Sala M and Castells X 2012 Inter- and intraradiologist variability in the BI-RADS assessment and breast density categories for screening mammograms *Br. J. Radiol.* **85** 1465–70
- Revol V, Kottler C, Kaufmann R, Straumann U and Urban C 2010 Noise analysis of grating-based x-ray differential phase contrast imaging *Rev. Sci. Instrum.* **81** 073709
- Shepherd J A, Kerlikowske K M, Smith-Bindman R, Genant H K and Cummings S R 2002 Measurement of breast density with dual x-ray absorptiometry: feasibility *Radiology* **223** 554–7
- Skaane P et al 2013 Comparison of digital mammography alone and digital mammography plus tomosynthesis in a population-based screening program *Radiology* **267** 47–56
- Stampanoni M, Wang Z, Thuring T, David C, Roessl E, Trippel M, Kubik-Huch R A, Singer G, Hohl M K and Hauser N 2011 The first analysis and clinical evaluation of native breast tissue using differential phase-contrast mammography *Invest. Radiol.* **46** 801–6

- Thompson D J *et al* 2009 Assessing the usefulness of a novel MRI-based breast density estimation algorithm in a cohort of women at high genetic risk of breast cancer: the UK MARIBS study *Breast Cancer Res.* **11** R80
- Van Engeland S, Snoeren P R, Huisman H, Boetes C and Karssemeijer N 2006 Volumetric breast density estimation from full-field digital mammograms *IEEE Trans. Med. Imaging* **25** 273–8
- Wang Z, Kang K, Huang Z and Chen Z 2009 Quantitative grating-based x-ray dark-field computed tomography *Appl. Phys. Lett.* **95** 094105
- Wang Z and Stampanoni M 2013 Quantitative x-ray radiography using grating interferometer: a feasibility study *Phys. Med. Biol.* **58** 6815–26
- Wernick M N, Wirjadi O, Chapman D, Zhong Z, Galatsanos N P, Yang Y, Brankov J G, Oltulu O, Anastasio M A and Muehleman C 2003 Multiple-image radiography *Phys. Med. Biol.* **48** 3875–95
- Wu X, Yan A and Liu H 2012 X-ray phase-shifts-based method of volumetric breast density measurement *Med. Phys.* **39** 4239–44
- Yaffe M J 2008 Measurement of mammographic density *Breast Cancer Res.* **10** 209
- Yaffe M J, Boone J M, Packard N, Alonzo-Proulx O, Huang S, Peressotti C L, Al-Mayah A and Brock K 2009 The myth of the 50–50 breast *Med. Phys.* **36** 5437–43